Petroleum and Coal

Article   Open Access

The Impact of Carbon Dioxide and Promotor Concentrations on Mass Transfer Characteristics in a Bubble Column Reactor

Ghassan H. Abdullah

Department of Chemical Engineering, Tikrit University, Iraq

Abstract

Developing a validated bubble column process that can be employed for design and optimization of the Benfield process is important to improve the process of gas sweetening in petrochemical process. In this work, the performance of chemisorption of carbon dioxide in amine promoted potassium carbonate solution in a bubble column reactor is studied using an electrochemical technique at different axial positions. Also, the effect of concentration of carbon dioxide and concentration of the promoter are investigated. It is found that the volumetric mass transfer coefficient increases rapidly for the same axial position with increasing carbon dioxide concentration. For the solution studied, the volumetric mass transfer coefficient, $K_L a$ is higher than that in K_2CO_3 solution at the same operation conditions. It has been found that the local volumetric mass transfer coefficient is obviously varied with the axial position. The mass transfer coefficient also decreases with a ratio of probe-to- distributor distance, this reduction became more significant in the promoted solution due to shrinkage of the bubbles.

Keywords: Amine promoted potassium carbonate; Bubble column; Electrochemical; Local mass transfer coefficient.

1. Introduction

Bubble columns are widely used in on commercial basis for mass transfer and reaction processes. These contactors are proved to be efficient in processing of two and three phase process for chemical and petrochemical industries [1]. They are specially used in low conversion processes to enhance the conversion and obtain high quality products such as polymers and alkylated products. It is also useful for oxidation, hydrogenation and hydrogenation processes. One of the common processes implemented in bubble columns is Fischer – Tropsch process that involve production of liquified fuel from coal and synthesis gas [2]. Also, Benfield process is a good candidate for utilizing bubble column as it involves chemisorption of carbon dioxide by potassium carbonate solution and mass transfer processes between gases (such as CO_2 and H_2S) and liquid are extensively present in this process. This process aims to remove hot and sour gases from the gas produced from gas reforming or refining of petroleum crude. Thus, it is required to intensively study the process and enhance the absorption and mass transfer processes. Electrochemical technique is recently used to measure the hydrodynamics of bubble column and focus locally on the parameters involved. Carbon dioxide and oxygen absorption is commonly used with electrical probes to measure mass transfer coefficient in aqueous solution [2]. Liquid mass transfer coefficient, $K_L a$, is the objective factor that is measured at the time of studying mass transfer in bubble column based on neglecting the gas side resistance. This coefficient is an important parameter for high precision design and scale up of the bubble column for this chemisorption process. The simulation model based on the bubble behaviors in bubble columns has been developed by Shimizu *et al.* [3]. The bubble break-up and coalescence which are the primary phenomena in bubble column reactors are taken into account to evaluate gas hold-ups and gas-liquid volumetric mass transfer rates. Krishna and Van Baten [4] developed a Computational Fluid Dynamic (CFD) model to describe mass

transfer for air-water bubble column operating in both homogeneous and heterogeneous regime. The later involves interaction of large and small gas bubbles that occupy part of the column namely gas holdup. Numerous researchers studied the system of this chemisorption. Darmana et al., [5] conducted a study that described simulations with an Euler–Lagrange model which takes into account mass transfer and chemical reaction reported by Darmana et al. [6]. The model was used to simulate the reversible two-step reactions found in the chemisorption process of CO_2 in an aqueous NaOH solution in a lab-scale pseudo-2D bubble column reactor. Before these reactions can take place, CO_2 gas first has to absorb in water physically: -

$$CO_2(g) \rightarrow CO_2(aq) \tag{1}$$

The elementary reactions than proceed as follows: -

$$CO_2(aq) + OH^- \overset{k_{1,2}}{\underset{k_{1,1}}{\Leftrightarrow}} HCO_3^- \tag{2}$$

$$HCO_3^- + OH^- \overset{k_{2,2}}{\underset{k_{2,1}}{\Leftrightarrow}} CO_3^{-2} \tag{3}$$
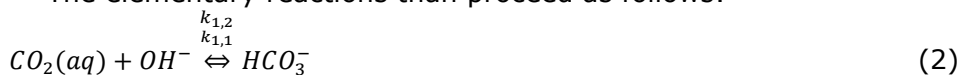
where $k_{1,1}$ and $k_{1,2}$, respectively, are the forward and backward rate constants for the first reaction while $k_{2,1}$ and $k_{2,2}$ represent the forward and backward rate constants for the second reaction.

It should be noted that the above correlations are valid when the volume of internals, commonly used in bubble column reactors (BCRs) and slurry bubble column reactors (SBCRs) for cooling or heating purposes, is ≤ 20% of the reactor volume. This is because several literature findings [7-15] showed limited or no effect of internals on the hydrodynamic and mass transfer parameters as long as their volume fraction remained under 20%. In addition, these correlations should be valid for reactor height/diameter ratio (HC/DC) range of 4-20, hence a considerable number of data points available in the literature [16-20] and used to develop these correlations cover such an HC/DC range. Dhaouadi et al., [21] studies the mass transfer behavior of gas- liquid experimentally in bubble column contactor. The contactor used was 6 m height and 0.15 m internal diameter. The liquid was water and the gas feed can be switched from air to nitrogen or vice versa. The classical 'gassing out' dynamic method is used to obtain the dissolved oxygen (DO) concentration profiles. An analytical description of the (DO) concentration evolution with time following the switch in the inlet gas is presented and allows the evaluation of the gas–liquid volumetric mass transfer coefficient for the different superficial gas velocities used.

Electrochemistry plays an important role today in many areas of science and technology as well as in our daily life-for example, in the development of batteries used in a vast range of consumer goods, in the manufacture and refining of many basic chemicals and in the preparation of potable water from brine through electrolysis. Furthermore, it becomes increasingly apparent that electrochemistry has the capacity to make an essential contribution to the solution of the energy and environmental problems now facing mankind. Just as the resistivity of a material is a characteristic property of that material, rather than the resistance itself, which contains contributions from purely geometrical factors, so we seek to define the conductivity for an electrolyte solution, which will be characteristic of that solution and independent of geometrical factors. The detailed theoretical background of this technique was described elsewhere [22]. Therefore, this technique is utilized in this study and validation is implanted to obtain the optimum condition that yield the highest mass transfer coefficient.

2. Experimental work

This part of research is carried out to obtain data of carbon dioxide absorption in Benfield solution. A bubble column apparatus was designed and installed to operate at different ranges of gas flow rates and liquor concentrations.

2.1 Material

Several chemicals were used in this study. Table 1 shows specifications of these chemicals.

Table 1. Specifications of chemicals

No.	Item	Specification
1	Potassium carbonate	Solid state, purity 99% (Sigma Aldrich)
2	Diethanolamine	Liquid state, purity 99% (Sigma Aldrich)
3	Carbon dioxide	Purity 99.5%(Manufacture : Iraqi Soft Drink Co.)
4	Nitrogen	Purity 99% (Sigma Aldrich)
5	HCl	Liquid state (Sd Fine- Chem. Limited, Mumbai)
6	Phenolphthalein	Solid state (BDH chemicals Ltd Poole, England)
7	Cupric carbonate	Solid state, (Sigma Aldrich)
8	KOH	Solid state (Cica KANTO Chemical Co. INC, Japan)
9	Bromocresol green	Solid state (BDH Chemicals Ltd Pole, England)
10	Vanadium	Liquid state, (Sigma Aldrich)

2.2. Experimental setup

The chemisorption study was conducted in a laboratory scale bubble column in a semi batch mode. The experimental setup is shown Figure 1. The core of the setup is the bubble column. The column is 6 cm x 6 cm rectangular section and 103 cm height fabricated from polymethyl-methacrylate sheets. The second component is the gas supply and stream and the third component is the electrical circuit. The gas mixture, carbon dioxide mixed to the desired concentration with nitrogen gas, is supplied from gas cylinders through an orifice (4 cm square pitch hole).
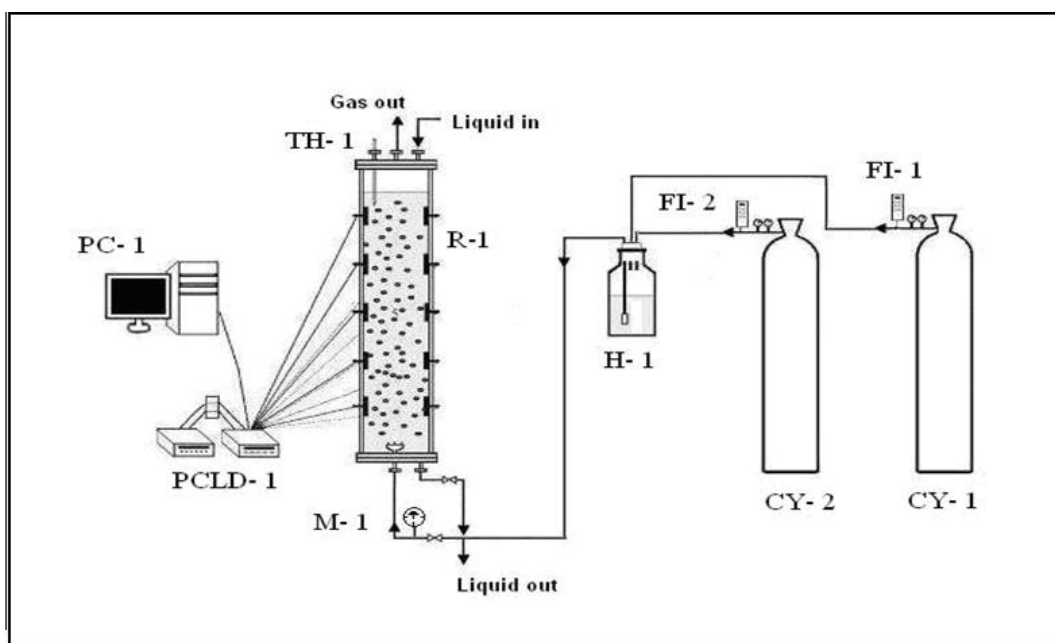
Figure.1 Experimental setup; CY- 1-CO_2 cylinder; CY- 2-N_2 cylinder; FI- 1-CO_2 gas flowmeter (0 - 500 L\ hr); FI- 2-N_2 gas flowmeter (0 – 40 L\ min); H – 1-Humidifier; M- 1-Gas manometer; R- 1-Bubble column reactor; TH- 1-Thermometer; PC- 1-Computer; PCLD- 1-Terminal Wiring Board

Prior to chemisorption in the bubble column, the gas mixture was feed to a humidifier to equalize the gas temperature and approach room temperature before flowing to the column. The flow of the gas mixture was controlled by gas flow meter. A pressure regulator was fixed at the inlet and the outlet of the gas mixture to control the pressure. The pressure and temperature were held constant (room and atmospheric temperature and pressure respectively) through the experiments. The initial height of liquid solution (potassium carbonated, promoted and unpromoted) was 100 cm above the distributor. The probes used for measuring local mass transfer coefficients along the height of the column is powered by a programmed electrical network. The network consists of electrical sine wave generator (1 kHz) junketed in series

with an electrical switching board and universal resistance and two probes at each axial position. The frequency of the wave generator (1 kHz) was selected after a preliminary experiment to reduce polarization between each pairs of the electrodes.
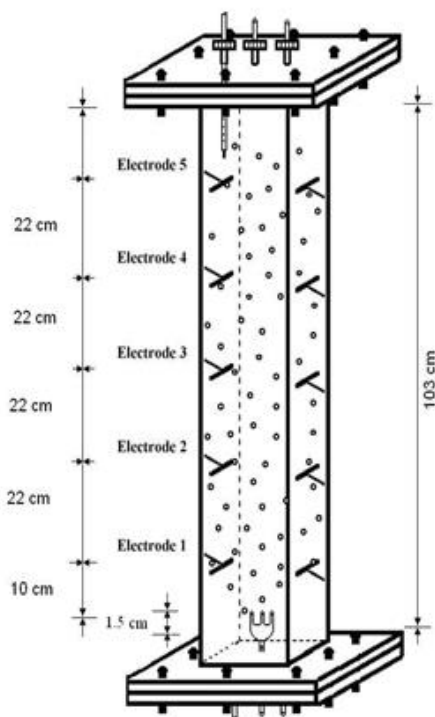
Figure2. Electrode positing on bubble column

The pairs of the electrodes were positioned at five different axial levels, the first pair was positioned 10 cm above the distributor and the next pairs were 22 cm distance from each other. The positioning of these pairs is shown in Figure 2. To run the build the electrical circuit, two stainless steel square plates were used as anode and cathode. The back faces of these plates were painted with an isolation paint to prevent contact with absorption solution. The plates were attached to the wall of the column by stainless steel screws painted with the same isolation paint. LabVIEW (Laboratory Virtual Instrument Engineering Workbench) was used in this study as a graphical programming language to create the applications. An interface was built by a set of tools and objects in LabVIEW to control BCR system. This interface is known as a front panel. Codes were added by a graphical representation of functions to control the front panel objects. This graphical source code was known as G code or block diagram code. The block diagram contains this code. In some ways, the block diagram resembles a flowchart.

For data acquisition, an interface was used and connected to each pair of electrodes (PCLD-8712 multifunction cards with 68-pin SCSI-II connectors, ADVANTECH, Taiwan) via a 2 m PCL-10168-2E 68-pin SCSI shielded cable. The electrodes were connected to the interface via a differential connection contains number of channels (n) named as 0, 2, 4, 6 and 8. The PCLD-8710 provides on- board Cold Junction Compensation (CJC) for the thermocouple measurement. Through setting of jumpers JP_0 and JP_1, control of the CJC circuitry and differential mode was obtained. For example, disabling mode of the jumper was shown in Figure.3a. A technical diagram of the PCLD-8710 Screw-terminal Board is shown in Figure.3b. LAB VIEW-Software Windows 8 was used to read voltage changes at the time of CO_2 absorption by Benfield solution. Calibration of the electrical circuit is implemented by a 1.5 V battery of a multimeter (Metaix, MX 553, France). The multimeter was connected to each of electrode pairs in the BCR (R-1), the reading on LAB VIEW screen should give the same voltage of the battery. Readings were taken at each of the five electrode pair in R-1, the value was 4.5 mA. The concentration of potassium carbonate solution was prepared at the desired value according to the plan of experiments. For this preparation at each concentration, the solution was titrated against 0.1 N hydrochloric acid and methyl red was used as an indicator to obtain the end point. R-1 is filled with the potassium carbonate solution up to 100 cm above the distributor. The flow meters of CO_2 and N_2 gases were calibrated prior to experimentation, the molar flow rate for the gas mixture was kept constant at 0.86×10^{-4} mol/s. To approach a steady state condition, a circulation for 10 min was conducted to obtain a precise reading on the data logger before flowing of gas mixture. Each experiment lasts for 35 minutes. The five channels were scanned and recorded the data every 60 sec [23-24], the electrical signal was transferred via the copper wire to the software of data acquisition (Lab View). Table 2 shows a sample of data collected at different heights along the column.

a.

b.

Figure 3. The PCLD-8710 Screw-terminal board
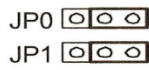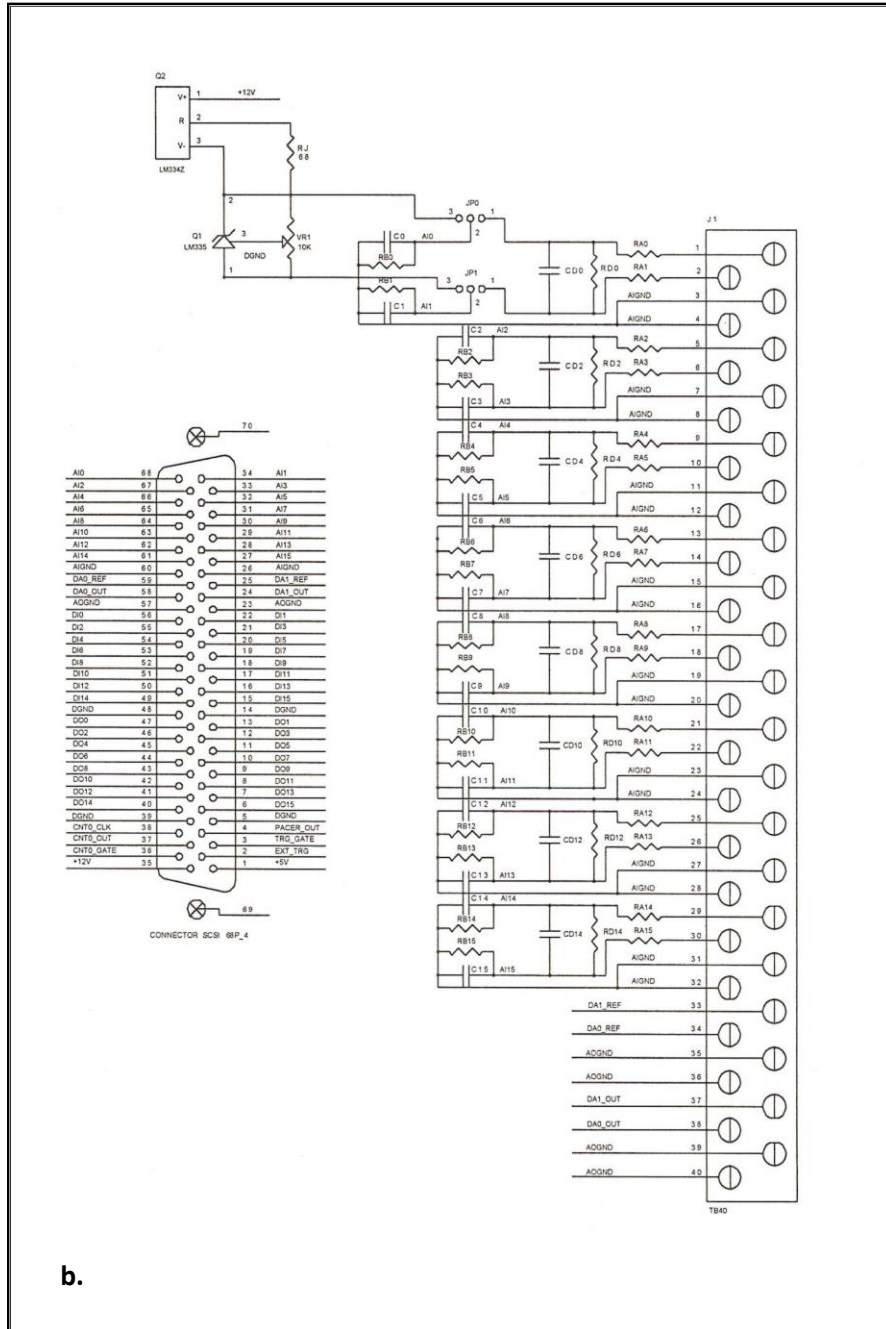
Table 2. Sample of experimental Voltage reading at 0.1 CO_2 fraction, $C_{K_2CO_3}$ = 0.5 M and C_{DEA}=0.0 M

Time (sec)	Voltage (V)				
	H_C=10 cm	H_C=32 cm	H_C=54 cm	H_C=76 cm	H_C=98 cm
0	0.020451	0.020451	0.020451	0.020451	0.020451
60	0.046930	0.043326	0.037829	0.032856	0.022393
120	0.047998	0.043783	0.038286	0.033873	0.024630
180	0.053644	0.046835	0.044237	0.037464	0.029971
240	0.056843	0.052630	0.047140	0.040085	0.037357
300	0.056848	0.052633	0.047136	0.040094	0.037362
360	0.059900	0.055990	0.047289	0.042927	0.037814
420	0.061884	0.057138	0.052019	0.046854	0.039001
480	0.062189	0.059653	0.055224	0.047886	0.041595
540	0.067835	0.064230	0.055834	0.048227	0.044189
600	0.074748	0.068503	0.061965	0.050668	0.045152
660	0.076990	0.073233	0.064837	0.053873	0.047423
720	0.078308	0.073538	0.065752	0.057704	0.049072
780	0.084385	0.076132	0.072313	0.057894	0.055633
840	0.089502	0.077200	0.073687	0.058908	0.056701
900	0.093927	0.080557	0.073992	0.061807	0.056854
960	0.098505	0.082998	0.077729	0.065775	0.062194
1020	0.099573	0.089408	0.077959	0.075998	0.070129
1080	0.101709	0.097424	0.087115	0.077371	0.070739
1140	0.102377	0.098105	0.091845	0.084543	0.071960
1200	0.105674	0.100695	0.092302	0.085001	0.073943
1260	0.114546	0.108026	0.095775	0.093494	0.079131
1320	0.117788	0.108942	0.100412	0.095837	0.087066
1380	0.125265	0.112298	0.110918	0.105447	0.088864
1440	0.127096	0.116113	0.115496	0.108194	0.093050
1500	0.129020	0.120996	0.118292	0.109857	0.106650
1560	0.131468	0.128073	0.124427	0.119943	0.106956
1620	0.132328	0.127959	0.125282	0.121164	0.107261
1680	0.132598	0.130985	0.129543	0.125284	0.116111
1740	0.133491	0.131976	0.131284	0.128800	0.119635
1800	0.134042	0.132761	0.131985	0.129033	0.121921

To obtain mass transfer coefficients, conductivity was utilized at each experiment for the carbon dioxide absorbed in potassium carbonate solution as the solution becomes conductive after chemisorption of carbon dioxide. Thus, the ionic concentration in solution (proportional to absorbed CO_2) can be obtained using the Debye –Hückel law [25].

$$\lambda = \lambda_O - K\sqrt{C_{CO_2}} \qquad (4)$$

where λ is conductivity and C_{CO_2} is the bulk ionic concentration; λ_o and K are two parameters, which are obtained experimentally by a calibration procedure that allows direct reading of the absorbed CO_2 in the present study.

The calibration procedure was conducted as follows:

1- Different concentrations of aqueous Benfield solutions 250 mL were prepared and divided into 50 mL aliquots, each in a separate beaker.
2- Carbon dioxide was bubbled into each aliquot for different times to obtain a concentration range of the absorbed CO_2 (from zero to saturation).
3- Each aliquot is characterized for conductivity measurement using a conductivity meter (Lovibond, con200, Germany), and absorbed CO_2 was determined by titration according to the following procedure.
   a. 20 mL of the sample from the spent absorbent is weighed, W.
   b. The sample was diluted to 250 mL with a distilled water.
   c. Accurately withdrawn 10 mL of aliquot sample and dilute to 100 mL with distilled water.

    d. Four drops of phenolphthalein were added as an indicator and a titration was con-
ducted by 0.1 N HCl till approaching a pH of 8. Thermo Orion, 410 A, USA was used
to measure the pH the acidity (V_P) was recorded.

    e. Four drops of bromocresol green indicator were added and titration was resumed till
pH drop to 3.8. The total acidity, V_t, was recorded.

$$\%KHCO_3 = 100.1 \left[\frac{0.1(V_t - 2V_P)}{W} \times \frac{25}{10} \times f_c - 0.00571\%DEA \right] \qquad (5)$$

$$CO_2 absorbed = \frac{1}{2}[KHCO_3] \qquad (6)$$

The concentration and weight percent of diethanolamine can be determined as follows:

1. 10 mL of the absorption product sample was poured in a 100 mL conical flask.
2. Potassium hydroxide solution (10%) was added to sample, cupric carbonate powered was
added (little amount only) and the volume was completed to 100 mL and mixed thoroughly
for 30 minutes.
3. Preparation of standard and blank solution
4. The absorbance was measured at 650 nm in a computerized UV- spectrophotometer (Jasco
530, manufacturer Jasco, Japan) of the sample (S_{AM}) and standard (S_T) against the blank
solution, and the weight percent of diethanolamine was calculated;

$$\%DEA = \frac{K_O}{S_T} \times S_{AM} \times \frac{25}{(W_t x 10)} \qquad K_O = 10 \qquad (7)$$

$$\%DEA = \frac{10}{S_T} \times S_{AM} \times \frac{25}{(W_t x 10)} \qquad (8)$$

For high precision, all tests were conducted in duplicate. The experimental conductivities
and the corresponding values of the CO_2 concentrations were substituted in equation 1 to
determine λ_o and K parameters. The obtained values are given in Table 3.

Table 3. Parameters of equation 1

Concentration of K_2CO_3 kmol/m^3	Concentration DEA kmol/m^3	Parameter K (S.cm^{-1}(kmol/m^3)$^{-1/2}$)	Parameter λ_o (S/cm)	Regression coefficient
0.5	0	7.2175	11.3970	0.9304
1	0	9.6185	20.6950	0.9831
1.5	0	10.2600	32.6430	0.9414
2	0	10.3070	39.8540	0.8669
2.5	0	6.8157	47.8030	0.8962
0.5	0.2	2.9086	13.9430	0.9008
1	0.2	7.3642	22.9450	0.9098
1.5	0.2	3.4435	35.4470	0.9333
2	0.2	3.8782	41.2600	0.9688
2.5	0.2	5.9812	51.3750	0.9957
0.5	0.3	7.8288	15.2240	0.9624
1	0.3	7.3240	25.7660	0.9249
1.5	0.3	3.3120	37.3660	0.9418
2	0.3	3.1759	44.5370	0.9298
2.5	0.3	3.1332	54.7870	0.9503

3. Results and discussion

Series of experiments were conducted to determine the overall and local volumetric mass
transfer coefficients in BCR by electrochemical technique. The data obtained at each electrode
pair were utilized to reveal differential trends and behavior. For instance, data from electrodes
at specific location were used to reveal local mass transfer coefficient differences as a function
of Benfield concentration and carbon dioxide mole fraction in gas phase. All the experiments
were carried out at constant molar flow rate of $CO_2 = 0.75 \times 10^{-5}$ kmol/s.

3.1. Influence of CO_2 mole fraction

Figures. 4 through 8 show the impact of mole fraction of CO_2 on local volumetric mass
transfer coefficient, K_La at different concentration of absorbent (promoted and un-promoted

potassium carbonate) along the height of BCR. Generally, they showed that the local K_La increases with increasing of the carbon dioxide mole fraction at the same axial position. This finding disagreed with Higbie's theory [25] and showed a positive effect of gas concentration on the volumetric mass transfer coefficient, K_La. The difference between values of local K_La along the height of the column is more obvious in Figures. 5 and 6 where the concentration of K_2CO_3 is greater than 0.5 M. Larger K_La values were obtained near the sparger, this coincided with the findings reported by Shimizu *et al.*, [3]. Moreover, K_La decreased with increasing HC/DC and this decrease is faster at higher mole fraction of CO_2. This may attribute to variation of bubble size and number of bubbles axially. These figures indicated that the use of a higher CO_2 mole fraction resulted in a faster consumption of the DEA in the aqueous solution due to the absorption process accompanied by a chemical reaction.
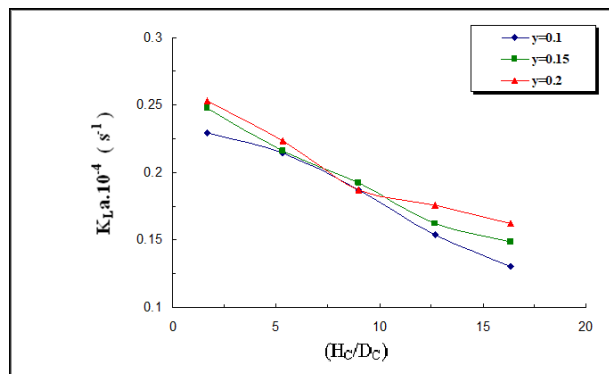
Figure 4. Effect of height to diameter ratio on local liquid mass transfer coefficient of carbon dioxide absorbed in 0.5 M potassium carbonate
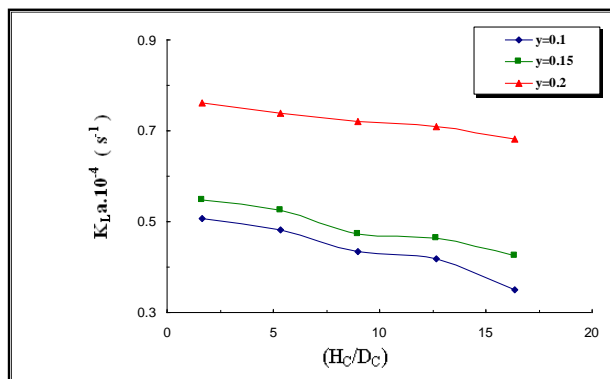
Figure 5. Effect of height to diameter ratio on local liquid mass transfer coefficient of carbon dioxide absorbed in 0.1 M potassium carbonate
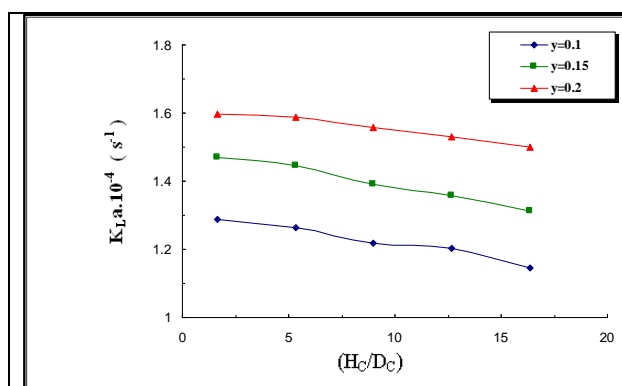
Figure 6. Effect of height to diameter ratio on local liquid mass transfer coefficient of carbon dioxide absorbed in 1.5 M potassium carbonate.
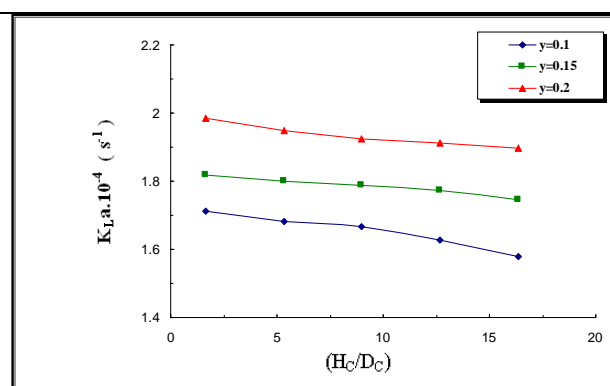
Figure 7. Effect of height to diameter ratio on local liquid mass transfer coefficient of carbon dioxide absorbed in 2 M potassium carbonate
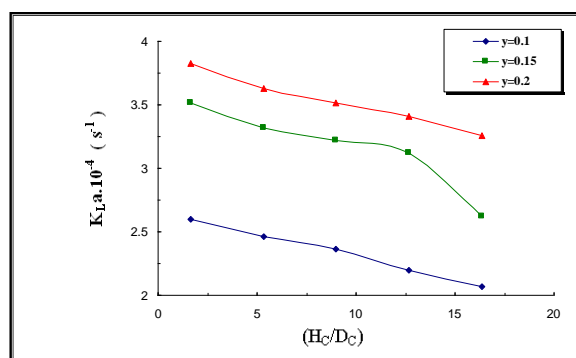
Figure 8. Effect of height to diameter ratio on local liquid mass transfer coefficient of carbon dioxide absorbed in 2.5 M potassium carbonate

3.2. Influence of promotor

The local K_La decreased with increasing HC/DC faster in the promoted potassium carbonate (Figures. 9 through 18). These results are in agreement with the results of Rocio *et al.*, [26-27], Verma *et al.*, [28] and Chaumat *et al.*, [29]. The decrease at low mole fraction of CO_2 is caused by a rapid consumption of the carbon dioxide concentration in the chemical reaction. At different CO_2 mole fraction, it is found that the volumetric mass transfer coefficient, K_La increased rapidly with increasing of the absorbent concentration (promoted potassium carbonate) at the same axial position.
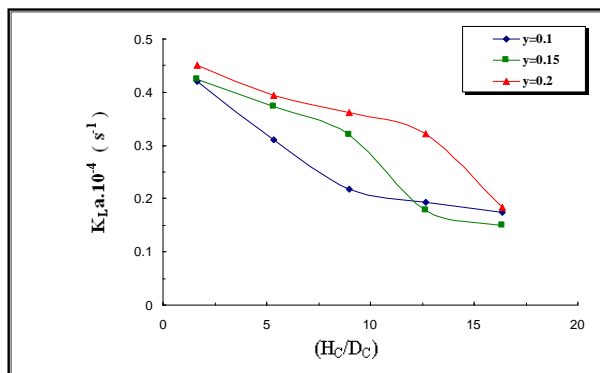
Figure 9. Effect of height to diameter ratio on local liquid mass transfer coefficient of CO_2 absorbed in 0.5 M K_2CO_3 and 0.2 M diethanol amine
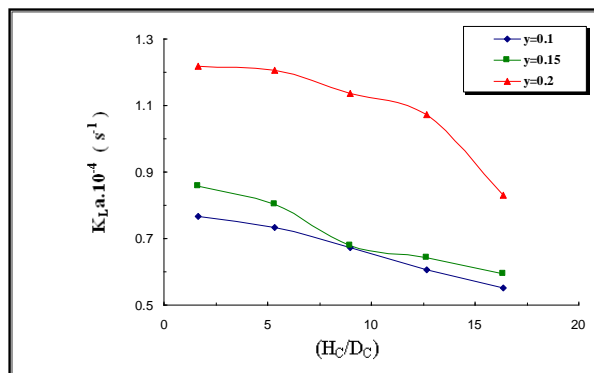
Figure 10. Effect of height to diameter ratio on local liquid mass transfer coefficient of CO_2 absorbed in 1 M K_2CO_3 and 0.2 M diethanol amine
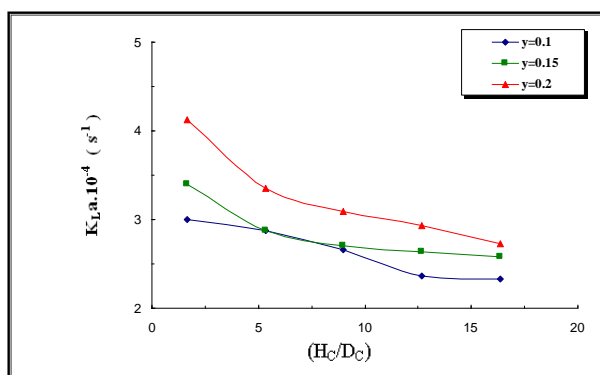
Figure 11. Effect of height to diameter ratio on local liquid mass transfer coefficient of CO_2 absorbed in 1.0 M K_2CO_3 and 0.2 M diethanol amine
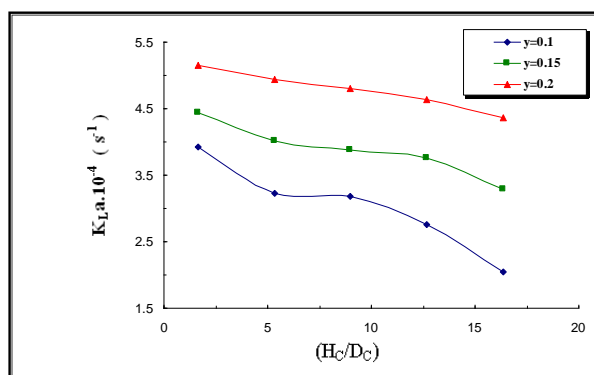
Figure 12. Effect of height to diameter ratio on local liquid mass transfer coefficient of CO_2 absorbed in 2.0 M K_2CO_3 and 0.2 M diethanol amine
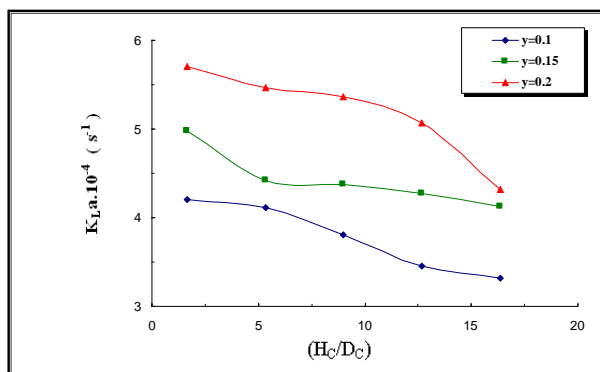
Figure 13. Effect of height to diameter ratio on local liquid mass transfer coefficient of CO_2 absorbed in 2.5 M K_2CO_3 and 0.2 M diethanol amine
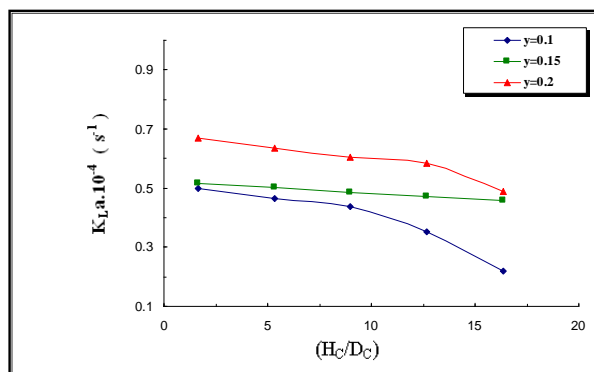
Figure 14. Effect of height to diameter ratio on local liquid mass transfer coefficient of CO_2 absorbed in 0.5 M K_2CO_3 and 0.3 M diethanol amine
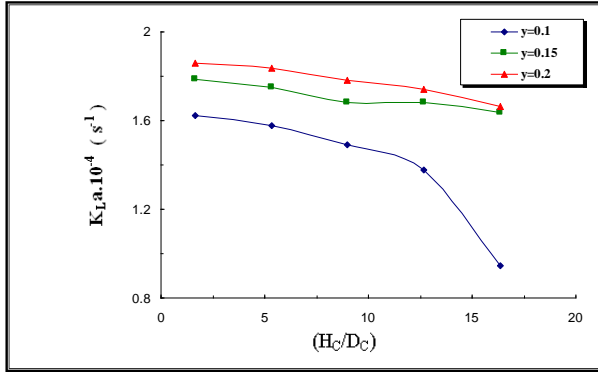
Figure 15. Effect of height to diameter ratio on local liquid mass transfer coefficient of CO_2 absorbed in 1.0 M K_2CO_3 and 0.3 M diethanol amine
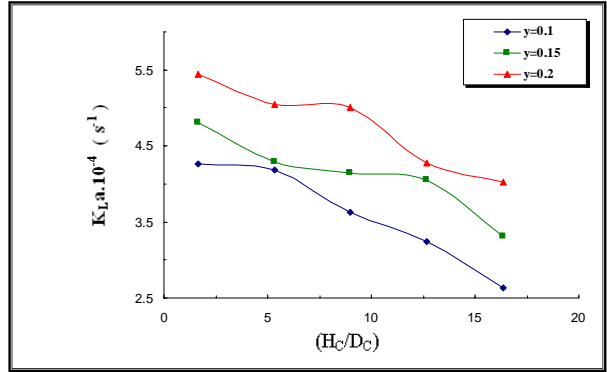
Figure 16. Effect of height to diameter ratio on local liquid mass transfer coefficient of CO_2 absorbed in 1.5 M K_2CO_3 and 0.3 M diethanol amine
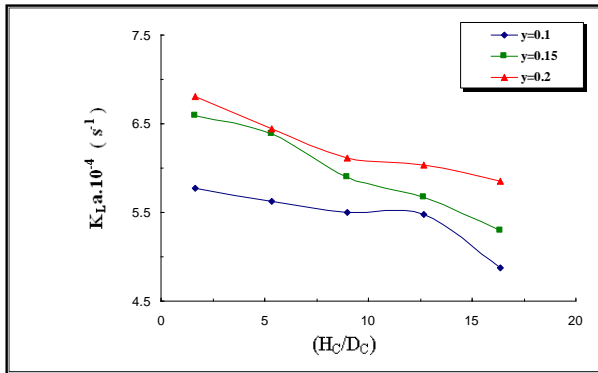
Figure 17. Effect of height to diameter ratio on local liquid mass transfer coefficient of CO_2 absorbed in 2.0 M K_2CO_3 and 0.3 M diethanol amine
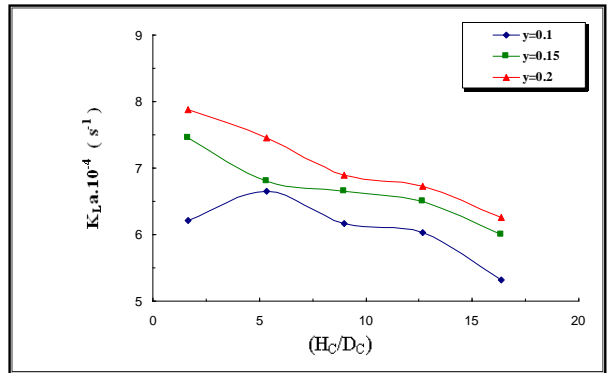
Figure 18. Effect of height to diameter ratio on local liquid mass transfer coefficient of CO_2 absorbed in 2.5 M K_2CO_3 and 0.3 M diethanol amine

When DEA is added to the solution, the absorption rate of CO_2 was enhanced significantly according to the following reactions [30]:

$$CO_2 + R_2NH \overset{K_{DEA}}{\Leftrightarrow} R_2N^+HCOO^- \tag{9}$$
$$R_2N^+HCOO^- + OH^- \Leftrightarrow R_2NH + HCO_3^- \tag{10}$$

Thus, very fast reaction of OH^- with DEA occurred and a Zwitterion intermediate is produced as shown in reactions 7 and 8 to regenerate DEA by reacting carbamate with OH^- which then diffuses back to the interface to react with more CO_2 molecules. These results are in agreement with the results of Rahimpour *et al.*, [31] Astarita *et al.*, [32], Dhotre *et al.*, [33], Dang-Vu *et al.*, [34], Arzutug *et al.*, [35], Goldstein *et al.*, [36] and Cullinane [37]. They proposed that the addition of an amine increases the reaction rate dramatically, consequently K_La increases. Increasing absorption rate and the volumetric mass transfer coefficient, K_La in promoted potassium carbonate solution is greater than that in un- promoted solution at the same concentration, owing to the fact that the reaction rate of K_2CO_3 solution is not high enough to dissolve CO_2 and destroyed the molecules chemically at the thin region near the interface.

These figures can show also that the volumetric mass transfer coefficient, K_La decreases with the increase in the electrode-to-sparger distance (H_C/D_C) for all concentration of potassium carbonate. As seen from these figures that this decreasing is more rapid at high concentration of potassium carbonate and low carbon dioxide mole fraction. The reason is mainly due to the rapid consumption of carbon dioxide concentration along the distance of the bubble column reactor.

This indicated that the rate of reaction and the volumetric mass transfer coefficient, $K_L a$ in a promoted potassium carbonate solution is higher than that in un-promoted potassium carbonate, as shown in Table 4. These figures indicate that the local $K_L a$ increases rapidly with increasing absorbent concentration (potassium carbonate) at the same axial position. The reason behind this increase is mainly attributed to the fact that the diffusion of the solute (gas) through the gas film is followed by diffusion through a liquid film of a variable thickness to a zone in which reaction between solute and absorbing liquid occurs. Thereby, the reaction zone at the gas–liquid interface decreases rapidly. Decreasing the thickness of the liquid film through the solute is due to increase OH^- concentration that reacts with carbon dioxide. Thus, the reaction step becomes dominant (equation 2) which is determined by OH^- concentration.

Table 4. Absorption rate of carbon dioxide measured at 300 sec.

Exp No.	y	$C_{K_2CO_3}$ Wt%	C_{DEA} Wt%	R_{CO_2} x 10^6 (kmol m^{-3} s^{-1})				
				H_C =10cm	H_C =32cm	H_C =54cm	H_C =76cm	H_C =98cm
1	0.1	5	0	0.002949	0.002947	0.002945	0.002938	0.002937
2	0.1	10	0	0.004709	0.004704	0.004702	0.004701	0.004700
3	0.1	15	0	0.013520	0.013519	0.013517	0.013516	0.013513
4	0.1	20	0	0.018282	0.018280	0.018280	0.018277	0.018274
5	0.1	25	0	0.125957	0.125663	0.125478	0.125148	0.124911
6	0.15	5	0	0.002930	0.002928	0.002927	0.002924	0.002920
7	0.15	10	0	0.005181	0.005181	0.005180	0.005178	0.005175
8	0.15	15	0	0.015533	0.015531	0.015527	0.015525	0.015521
9	0.15	20	0	0.019279	0.019277	0.019276	0.019275	0.019272
10	0.15	25	0	0.198193	0.197189	0.196690	0.196204	0.193991
11	0.2	5	0	0.002599	0.002597	0.002594	0.002594	0.002592
12	0.2	10	0	0.009064	0.009064	0.009063	0.009063	0.009062
13	0.2	15	0	0.017201	0.017200	0.017197	0.017193	0.017190
14	0.2	20	0	0.018238	0.018234	0.018231	0.018230	0.018229
15	0.2	25	0	0.203184	0.201958	0.201290	0.200641	0.199786
16	0.1	5	2	0.005237	0.005236	0.005236	0.005233	0.005230
17	0.1	10	2	0.023060	0.023058	0.023054	0.023050	0.023047
18	0.1	15	2	0.487089	0.482989	0.476623	0.468504	0.467447
19	0.1	20	2	0.769950	0.737635	0.735488	0.718174	0.694702
20	0.1	25	2	0.256046	0.255179	0.252579	0.249687	0.248706
21	0.15	5	2	0.011596	0.011595	0.011594	0.011592	0.011592
22	0.15	10	2	0.022380	0.022376	0.022366	0.022364	0.022361
23	0.15	15	2	0.675876	0.650613	0.643047	0.640041	0.637516
24	0.15	20	2	0.834233	0.808605	0.799924	0.793710	0.768183
25	0.15	25	2	0.283294	0.277606	0.277219	0.276266	0.274780
26	0.2	5	2	0.009808	0.009807	0.009807	0.009806	0.009805
27	0.2	10	2	0.032058	0.032057	0.032044	0.032032	0.031997
28	0.2	15	2	0.847611	0.789778	0.772186	0.761883	0.749592
29	0.2	20	2	0.957173	0.940698	0.930429	0.916481	0.896919
30	0.2	25	2	0.363829	0.359675	0.357787	0.352947	0.341415
31	0.1	5	3	0.015633	0.015632	0.015631	0.015629	0.015626
32	0.1	10	3	0.044927	0.044914	0.044885	0.044853	0.044749
33	0.1	15	3	1.055675	1.048786	1.005399	0.978590	0.941092
34	0.1	20	3	2.166938	2.137783	2.113215	2.111337	2.002064
35	0.1	25	3	3.697045	3.867264	3.683515	3.631987	3.378291
36	0.15	5	3	0.015638	0.015637	0.015637	0.015637	0.015636
37	0.15	10	3	0.049902	0.049884	0.049851	0.049851	0.049833
38	0.15	15	3	1.321772	1.261227	1.244432	1.234537	1.158804
39	0.15	20	3	2.601149	2.553652	2.435012	2.384143	2.298408

Exp No.	y	$C_{K_2CO_3}$ Wt%	C_{DEA} Wt%	R_{CO_2} x 10^6 (kmol m^{-3} s^{-1})				
				H_C =10cm	H_C =32cm	H_C =54cm	H_C =76cm	H_C =98cm
40	0.15	25	3	4.604870	4.325534	4.263234	4.197329	3.995324
41	0.2	5	3	0.015511	0.015509	0.015508	0.015507	0.015504
42	0.2	10	3	0.048844	0.048833	0.048802	0.048782	0.048743
43	0.2	15	3	1.423913	1.370256	1.363639	1.272387	1.241482
44	0.2	20	3	2.550414	2.462810	2.387596	2.366719	2.325351
45	0.2	25	3	5.507661	5.290844	5.003258	4.912236	4.683158

4. Conclusions

The volumetric mass transfer coefficient, K_La increases rapidly at the same axial position when: *i.* increasing absorbent concentration (potassium carbonate); *ii.* increasing DEA promoter concentration; *iii.* increasing of the carbon dioxide mole fraction.

The volumetric mass transfer coefficient, K_La decreases with the increase in the electrode-to-sparger distance (H_C/D_C) when: *i.* increasing absorbent concentration (potassium carbonate); *ii.* increasing DEA promoter concentration; *iii.* increasing of the carbon dioxide mole fraction; *iv.* as the bubble rises along the column due to bubble shrinkage.

The zwitterion mechanism is found to fit the experimental data very well. The results indicate that the reaction rate and the volumetric mass transfer coefficient, K_La in promoted potassium carbonate (Benfield solution) is higher than that in un-promoted potassium carbonate.

The results of the present work provide a new methodology for gas–liquid mass transfer studies. It has been demonstrated that the volumetric mass transfer coefficient is a function of column height which validated the findings of previous studies used conventional methods.

The empirical model proposed in the present study is allows for the prediction of the local mass transfer coefficient at specific locations in the column height as a function of the solution.

The results for the local volumetric mass transfer coefficient, K_La are not coincides with the assumption of a constant mass transfer coefficient throughout the bubble column reactor. K_La is found to vary with the axial position in the bubble column reactor.

References

[1]   Degaleesan S, Dudukovic M, Pan. Y. AIChE J., 2001; 47: 1913-31.
[2]   Nigar K, Fahir B, Kutlu O. Process Biochemistry, 2005; 40: 2263–2283.
[3]   Shimizu K, Takada S, Minekawa K, Kawase Y. Chem. Eng. J., 2000; 78: 21–28.
[4]   Krishna R, van Baten, JM Catalysis Today, 2003; 79–80: 67–75.
[5]   Darmana D, Henket RLB, Deen NG, Kuipers JAM. Chem. Eng. Sci., 2007; 62: 2556 – 2575.
[6]   Darmana D, Deen NG, Kuipers JAM. Chem. Eng. Sci., 2005; 60: 3383 – 3404.
[7]   Saxena SC, and Chen ZD. Rev. Chem. Eng., 1994; 10(3–4): 193–400.
[8]   Dowd WO, Smith DN, Ruether JA, Saxena SC. AIChE J., 1987; 33(12): 1959–1970.
[9]   Saxena SC, Rao NS, Thimmapuram PR. Chem. Eng. J., 1992; 49(3): 151–159.
[10]   Shah YT, Ratway CA, McIlvried HG. Trans. Inst. Chem. Eng., 1978; 56 (2): 107–112.
[11]   Joseph S. Unpublished Ph.D. Thesis, University of Pittsburgh 1985, Pittsburgh, USA.
[12]   Yamashita F. Chem. Eng. J., 1987; 20(2): 204–206.
[13]   Chen J, Li F, Degaleesan S, Gupta P, Al-Dahhan MH, Dudukovic MP, Toseland BA. Chem. Eng. Sci., 1999; 54(13–14): 2187–2197.
[14]   De SK, Ghosh S, Parichha RK, De P. Indian Chem. Eng., 1999; 41(2): 112–116.
[15]   Forret A, Schweitzer JM, Gauthier T, Krishna R, Schweich D. Can. J. Chem. Eng., 2003; 81(3–4): 360–366.
[16]   Vermeer DJ, and Krishna R. Ind. Eng. Chem. Process, 1981; 20(3): 475–482.
[17]   Eickenbusch H, Brunn PO, Schumpe A. Chem. Eng. Process., 1995; 34(5): 479–485.
[18]   Moustiri S, Hebrard G, Thakre SS, Roustan M. Chem. Eng. Sci., 2001; 56(3): 1041–1047.
[19]   Guy C, Carreau PJ, Paris J. Can. J. Chem. Eng., 1986; 64(1): 23–35.
[20]   Pino LZ, Solari RB, Siquier S, Estevez LA, Yepez MM, Saez AE. Chem. Eng. Commun., 1992; 117: 367–382.
[21]   Dhaouadi H, Poncin S, Hornut JM, Midoux N. Chem. Eng. and Processing, 2008; 47: 548–556.
[22]   Ghani SA, Khalefa IA. Petroleum Science and Technology, 2011; 29:1494–1503, 2011.
[23]   Rocio M, Sebastia SA, Cancela MA, Estrella A. Chem. Eng. J., 2008; 137: 422–427.

[24]   Cancela MA, Maceiras R, Álvarez E, Nóvoa XR. Proceedings of European Congress of Chemical Engineering (ECCE-6) Copenhagen, (2008) 16-20.
[25]   Maceiras R, Nóvoa XR, Álvarez E, Cancela MA. Chem. Eng. and Processing, 2007; 46: 1006–1011
[26]   Rocio M, Sebastia SA, Cancela MA, Estrella A. Chem. Eng. J., 2008; 137 : 422–427
[27]   Maceiras R, Nóvoa XR, Álvarez E, Cancela MA. Chem. Eng. and Processing, 2007; 46: 1006–1011.
[28]   Verma AK, Rai S. Chem. Eng. J., 2003; 94: 67–72.
[29]   Chaumat H, Billet-Duquennea AM, Augier F, Mathieu C, Delmas H. Chem. Eng. Sci.,2005; 60: 5930 – 5936.
[30]   Tseng PC and Savage DW. AlChE J., 1988; 34: 922-931.
[31]   Rahimpour MR, Kashkooli AZ. Iranian Journal of Science and Technology, 2004; 28: 655-667.
[32]   Astarita G, Savage WD, Longo JM. Chem. Eng. Sci., 1981; 36: 581.
33[]   Dhotre MT, Vitankar VS, Joshi JB. Chem. Eng. J., 2005; 108: 117-125.
[34]   Dang-Vu T, Doan HD, Lohi A. Industrial & Engineering Chemistry Research, 2006; 45: 1097-1104.
[35]   Arzutug ME, Yapici S, Muhtar Kocakerim M. International Communications in Heat and Mass Transfer, 2005; 32: 842–854.
[36]   Goldstein RJ, Chiang HD, Srinivasan V. International Communications Heat and Mass Transfer, 2005; 41: 991–998.
[27]   Cullinane JT, Rochelle GT. Chemical Engineering Science, 2004; 59, 17: 3619-3630.

To whom correspondence should be addressed: Dr. Saba A. Gheni. Department of Chemical Engineering, Tikrit University, Iraq, E-mail: ghassan.hamad10@gmail.com